

Phase space analysis of two-wavelength interferometry

Robert H. Leonard^{1,*} and Spencer E. Olson²

¹Space Dynamics Laboratory, Quantum Sensing & Timing, North Logan, UT 84341, USA

²Air Force Research Laboratory, Kirtland Air Force Base, NM 87117, USA

*robert.leonard@sdl.usu.edu

September 20, 2023

Abstract

Multiple wavelength phase shifting interferometry is widely used to extend the unambiguous range (UR) beyond that of a single wavelength. Towards this end, many algorithms have been developed to calculate the optical path difference (OPD) from the phase measurements of multiple wavelengths. These algorithms fail when phase error exceeds a specific threshold. In this paper, we examine this failure condition. We introduce a “phase-space” view of multi-wavelength algorithms and demonstrate how this view may be used to understand an algorithm’s robustness to phase measurement error. In particular, we show that the robustness of the synthetic wavelength algorithm deteriorates near the edges of its UR. We show that the robustness of de Groot’s extended range algorithm [1] depends on both wavelength and OPD in a non-trivial manner. Further, we demonstrate that the algorithm developed by Houairi & Cassaing (HC) [2] results in uniform robustness across the entire UR. Finally, we explore the effect that wavelength error has on the robustness of the HC algorithm.

1 Introduction

Determination of the absolute phase is important in applications such as interferometric synthetic aperture radar [3–5], strain/stress analysis [6], and atom interferometry [7]. Phase measurements are also critical in order to characterize a surface height via optical profilometry [8, 9], which can be used with a single wavelength or a more complex multiple-wavelength configuration.

Single-wavelength phase shifting interferometry measures the phase difference modulo 2π , resulting in an $n\lambda$ ambiguity in the optical path difference (OPD), where n is an integer and λ is the wavelength used. Consequently, the OPD may be unambiguously resolved when restricted to the range $\pm\lambda/2$; we refer to such a range as the unambiguous range (UR), and denote the length of the range as $|\text{UR}|$. Comparison of phase measurements from multiple wavelengths allows the UR to be extended beyond that of a single wavelength. Towards this end, many algorithms have been developed which incorporate phase measurements from multiple wavelengths to determine the absolute phase with a larger UR [1, 2, 10–12]. These algorithms will fail when the phase error exceeds a specific threshold.

In this paper we explore the conditions under which multi-wavelength algorithms are valid. In Sec. 2 we provide a brief derivation of the maximum UR achievable for an algorithm which uses two phase measurements. In Sec. 3 we introduce and characterize the phase space of multi-wavelength interferometry. In Sec. 4 we build on our understanding of the phase space to describe the effect that phase measurement error has on the accuracy of the measured OPD as well as the robustness of the algorithm. In Sec. 5 we show that the synthetic wavelength algorithm, where data from multiple wavelengths are combined together to create a single data set of larger synthetic wavelength Λ , creates an uneven partitioning of the phase space. This uneven partitioning results in a robustness which decreases when the OPD is within $\lambda_i/2$ of $\pm\Lambda/2$, where λ_i is any of the individual real wavelengths. We show that this decrease in robustness is the result of an overlooked constraint of the algorithm. In Sec. 6, we examine an algorithm created by de Groot [1]. While de Groot’s algorithm correctly calculates the OPD in the absence of phase measurement error, we find that the algorithm exhibits complicated behavior when phase error is present. An explanation for this behavior is presented. We show that the robustness of de Groot’s

algorithm will generally vary with OPD. The condition under which de Groot's algorithm achieves maximum robustness is described. In Sec. 7, we demonstrate that the Houairi & Cassaing algorithm evenly partitions the phase space, resulting in uniform robustness over nearly the entire UR. In Sec. 8 we examine the effect of wavelength error on the Houairi & Cassaing (HC) algorithm.

2 Maximum Unambiguous Range

We define the maximum UR as the largest range of OPD such that any two OPDs within this range are distinguishable when measurement error is absent. For an algorithm which uses a pair of phase measurements from two different wavelengths as input, two OPDs are indistinguishable when they result in the same measured phase pair (ϕ_a, ϕ_b) where a and b denote data from the different wavelengths. Therefore, the minimum distance between two OPDs which result in the same phase pair will equal the maximum UR. We will denote the OPD as d . To simplify the analysis, we will assume $\lambda_a > \lambda_b$ throughout.

Consider the measured phase pair $(0, 0)$. A phase measurement will equal zero when d equals an integer multiple of λ . Therefore, the phases pass through $(0, 0)$ when $d = n_a \lambda_a = n_b \lambda_b$ where $n_a, n_b \in \mathbb{Z}$. This Diophantine equation has a trivial solution at $d = 0$. Following the notation used by Houairi and Cassaing [2], we denote the next smallest integer pair which satisfies this equation as p, q . Therefore, the length of the maximum |UR| may be written as

$$|\text{UR}_{\max}| = p\lambda_b = q\lambda_a \quad (1)$$

where p, q are the co-prime natural numbers which satisfy the equation on the right side of Eq. 1. This result has been previously noted [11, 13].

Note that Eq. 1 is only satisfied when λ_a and λ_b are commensurate. When λ_a and λ_b are incommensurate, the measured phase pairs never repeat, resulting in an infinite UR. In practice, the maximum desirable UR will be constrained by measurement error [2].

3 Phase-Space Representation

For two-wavelength interferometry with wavelengths λ_a and λ_b , the measured phases in the absence of error are given by

$$\phi_i = \frac{2\pi d}{\lambda_i} \pmod{2\pi} \quad (2)$$

where $i \in \{a, b\}$, and \pmod is defined by the formula

$$a \pmod b := a - b \left\lfloor \frac{a}{b} \right\rfloor \quad (3)$$

and where $\lfloor x \rfloor$ denotes the nearest integer value to x .

Consider a graph in which ϕ_a and ϕ_b are plotted on the x and y axes respectively. In this representation, all measured phases fall within the space $(\phi_a, \phi_b) \in [-\pi, \pi) \times [-\pi, \pi)$; we call this *phase space*. In Fig. 1, we show ideal phase measurements plotted in phase space over the entire UR. This representation is easily constructed by parametrically plotting the phases using Eq. 2.

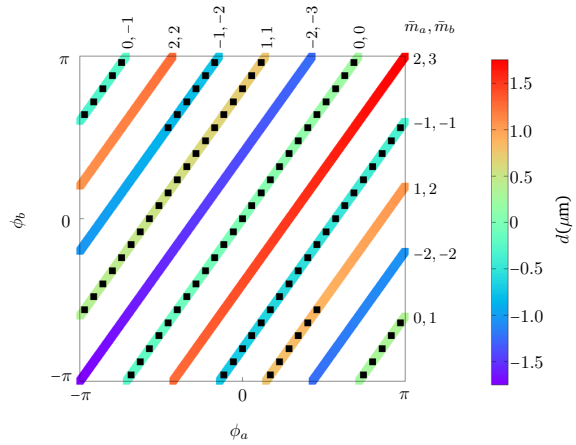


Figure 1: Ideal phase measurements for $\lambda_a = 700$ nm and $\lambda_b = 500$ nm over: the entire $3.5 \mu\text{m}$ UR (solid); the UR of the synthetic wavelength algorithm (square dots). The OPD (d) is represented by the color. At $d = 0 \mu\text{m}$ the phase is $(0, 0)$. As d increases the phases moves upwards along the $0, 0$ line. When $\phi_b = \pi$, the phases jump to the bottom of the $0, 1$ line. Starting from $-\text{UR}_{\max}/2$, and increasing in d , the ideal phases jump between the lines in the following order: $(-2 - 3)$, $(-2 - 2)$, $(-1, -2)$, $(-1, -1)$, $(0, -1)$, $(0, 0)$, $(0, 1)$, $(1, 1)$, $(1, 2)$, $(2, 2)$, $(2, 3)$.

Following the notation introduced in Ref. [2], we write the OPD (d) as follows

$$d = \lambda_a(\bar{m}_a + \hat{m}_a) = \lambda_b(\bar{m}_b + \hat{m}_b) \quad (4)$$

where $\bar{m} \in \mathbb{Z}$ and $\hat{m} \in [-0.5, 0.5]$. The value of \hat{m} is related to the measured phase by

$$\hat{m}_i = \frac{\phi_i}{2\pi}. \quad (5)$$

As shown in Fig. 1, as d increases from zero which is found at $(\phi_a, \phi_b) = (0, 0)$, the phases follow a line with slope $r_\lambda = \lambda_a/\lambda_b$ in the phase space. When ϕ_a or

ϕ_b reach $\pm\pi$, the phase “wraps back” to $\mp\pi$, creating a new line. This occurs when $\bar{m}_i = \pm 0.5$. The new line corresponds to the incremented value of \bar{m}_i . In this way, ideal phase measurements form a set of parallel lines where each line is uniquely associated with an integer pair (\bar{m}_a, \bar{m}_b) . When plotted over the entire UR, each line is displaced from the adjacent line by an equal amount. The displacement between adjacent lines is

$$\Delta\phi_i = \frac{2\pi\lambda_i}{|\text{UR}_{\max}|}. \quad (6)$$

4 Phase-Space View of Phase Errors

Building on our knowledge of the phase space, we can imagine a two-wavelength interferometry algorithm which achieves the maximal UR. When error is present, measured phases deviate from the lines shown in Fig. 1. Because each line is associated with a unique integer pair (\bar{m}_a, \bar{m}_b) , we can determine the values of \bar{m}_i by identifying the line closest to the measured phase pair (ϕ_a, ϕ_b) . Once the values of \bar{m}_i are known, the OPD (d) is determined using Eqs. 4 and 5. Brug and Klaver [13] developed an algorithm similar to this using a lookup table for all phase values in the phase space.

Phase measurement error effects interferometry algorithms in two ways: (1) phase error may result in an error in the calculated value of \bar{m}_i (a continuous variable); (2) phase error may result in the incorrect determination of \bar{m}_i (an integer variable). Because an incorrect determination of \bar{m}_i will result in a large error in the calculated OPD, we classify (2) as an algorithm failure and (1) as typical measurement error. It is helpful to think of the phase errors as a displacement vector in the phase space, $\vec{\delta\phi} = \langle \delta\phi_a, \delta\phi_b \rangle$ where $\delta\phi_i$ is the error in ϕ_i . When possible, it is helpful to decompose the phase error into components corresponding to these different effects. To this end, another convenient coordinate system for error decomposition is parallel and perpendicular to the ideal phase lines (e.g as shown in Fig. 1), denoted by $\vec{\delta\phi} = \langle \delta\phi_{\perp}, \delta\phi_{\parallel} \rangle$.

An algorithm will incorrectly determine \bar{m}_i when phase error displaces the phase from its ideal value so that the measured phase is closer to a line corresponding to incorrect values of \bar{m}_i . Consequently, $\delta\phi_{\perp}$ is responsible for algorithm failure, whereas $\delta\phi_{\parallel}$ is identified as simple measurement error.

Any two-wavelength algorithm which uses Eq. 4 will result in two OPD calculations. In general, when both calculated values for OPD are combined into a weighted average, the resulting error in the OPD will

depend on the phase error in a non-trivial way. For the special case in which both phase measurements have equal uncertainty, the weighted average of the two OPD results will correspond to a point exactly on the ideal phase line which is closest to the measured phase. In this case, $\delta\phi_{\parallel}$ is solely responsible for error in the calculated OPD. We will assume that both OPD results are combined into a weighted average for the remainder of this paper. When the phase uncertainties are the same for both wavelengths, $\delta\phi_{\parallel}$ is related to the error in d by

$$\delta d = \frac{\delta\phi_{\parallel}}{2\pi} \frac{\lambda_a \lambda_b}{\sqrt{\lambda_a^2 + \lambda_b^2}}. \quad (7)$$

$\langle \phi_a, \phi_b \rangle$ is related to $\langle \phi_{\parallel}, \phi_{\perp} \rangle$ by the rotational transformation

$$\langle \phi_{\parallel}, \phi_{\perp} \rangle^T = \mathcal{R}_{-\theta} \langle \phi_a, \phi_b \rangle^T \quad (8)$$

where θ is given by

$$\theta = \tan^{-1} \left(\frac{\lambda_a}{\lambda_b} \right) \quad (9)$$

and where $\mathcal{R}_{-\theta}$ is the typical rotation matrix about an angle $-\theta$.

Recall that an algorithm is deemed to have failed when the values of \bar{m}_i are determined incorrectly. We define robustness, R , as the probability that the algorithm will succeed. Robustness may be calculated by integrating the probability distribution function for the measured phase values over the range of phase values for which the algorithm returns the correct values of \bar{m}_i . For the remainder of this paper, we assume that measured phases deviate from ideal values according to a normal distribution with standard deviation equal to the measurement uncertainty, σ_i . As we see in the next section, the robustness may depend on the OPD.

Note that any algorithm which achieves the maximum UR will pass through the $(\pm\pi, \pm\pi)$ corners of the phase space when $d = \pm\text{UR}_{\max}/2$. Because measured phases are constrained to fall within $[-\pi, \pi)$, discontinuities in the measured phases arise near the $(\pm\pi, \pm\pi)$ corners (Fig. 4a can be used to visualize this). For instance: when $d = -\text{UR}_{\max}/2$, the phases should be $(-\pi, -\pi)$. A measurement error which would normally result in a small negative phase error, now results in a phase error of nearly $+2\pi$ (as measurement error can cause ϕ_a to wrap to the right of Fig. 4a or ϕ_b to wrap to the top of Fig. 4a). As a result, the robustness of an algorithm which achieves the maximum UR will deteriorate when the OPD is within measurement uncertainty of $\pm|\text{UR}_{\max}|/2$. Specifically, the robustness will

approach $1/4$ as $d \rightarrow \pm |\text{UR}_{\text{max}}|/2$. An algorithm will avoid this failure mode when both phase errors satisfy the constraint

$$\left| d_0 + \lambda_i \frac{\delta\phi_i}{2\pi} \right| < \frac{|\text{UR}_{\text{max}}|}{2}. \quad (10)$$

5 Synthetic Wavelength Algorithm

The synthetic wavelength algorithm was first introduced by J. C. Wyant [14]. The algorithm uses phase measurements from two wavelengths, λ_a and λ_b , to calculate the phase that would be produced by a larger synthetic wavelength, Λ , which is defined as

$$\Lambda = \frac{\lambda_a \lambda_b}{|\lambda_a - \lambda_b|}. \quad (11)$$

As a result, the synthetic wavelength algorithm has an UR of $\pm\Lambda/2$. A major benefit of phase measurements from an effectively longer wavelength is to simplify the phase-unwrapping by reducing the many 2π phase ambiguities. Additionally, a synthetic wavelength measurement produced from shorter wavelengths takes advantage of much easier optical elements, detectors, and cameras as compared to available resources for the longer wavelengths.

For most choices of wavelengths, the UR of the synthetic wavelength algorithm is less than the maximum UR that could be achieved for same choice of wavelengths (as described in Sec. 2). When ideal phase measurements are plotted over the UR of the synthetic wavelength algorithm, the resulting lines terminate before they can form a set of evenly spaced lines. An example of this is shown in Fig. 1 where the truncated UR of the synthetic wavelength algorithm (square dots) is compared to the ideal case (solid lines). The irregular spacing of these ideal phase lines hint that the robustness of the synthetic wavelength algorithm may vary with OPD.

Note that any two-wavelength algorithm may be thought of as a function which takes two phases as an input and returns an OPD; *i.e.* $\text{OPD} := d(\phi_a, \phi_b)$. With this in mind, and to further understand the behavior of the synthetic wavelength algorithm, the algorithm can be applied to a raster scan of phase values, ϕ_a and ϕ_b , across the entire phase space, $[-\pi, \pi) \times [-\pi, \pi)$. Fig. 2 shows the OPD as calculated using the synthetic wavelength algorithm for $\lambda_a = 700$ nm and $\lambda_b = 500$ nm by doing such a raster scan of phase space. As we will show below, the qualitative features seen in Fig. 2 are common to any choice of wavelength, even when the UR of the synthetic wavelength algorithm equals the maximum UR.

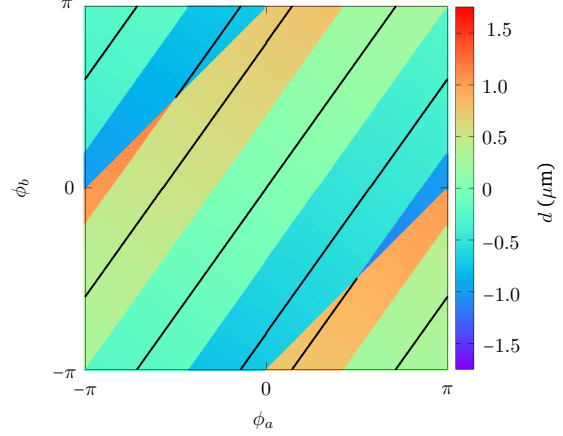


Figure 2: Calculated OPD (d) for $\lambda_a = 700$ nm and $\lambda_b = 500$ nm using the synthetic wavelength algorithm. The solid line shows the expected phase values when measurement error is absent—note that the solid line does not evenly fill the phase space, as occurs in Fig. 1. Similar to Fig. 1, the color scale represents OPD (d) and $d = 0$ μm occurs at $(\phi_a, \phi_b) = (0, 0)$.

The phase-mapping of OPD shown in Fig. 2 is characterized by continuous bands of OPD (d), where all points within each continuous region correspond to a unique pair (\bar{m}_a, \bar{m}_b) . The continuous bands of OPD are bounded by discontinuities in d that represent sudden changes in the values of \bar{m}_i . When the the OPD is within the algorithm's UR, and measurement error is absent, the measured phases (ϕ_a, ϕ_b) lie exactly on the ideal phase (solid) lines shown in Fig. 2, and the values of \bar{m}_i are easily resolved. When error is present, the measured phase is displaced from the ideal phase; as long as the displacement is small enough to remain within the same continuous band, the values of \bar{m}_i are resolved correctly. On the other hand, when the measured and ideal phases are separated by a discontinuity boundary, the values of \bar{m}_i are incorrectly resolved.

Near $d = 0$, the discontinuities in the calculated OPD are parallel to the ideal phase lines, and the ideal phase lines are evenly spaced. This appears to be a common feature of all two-wavelength interferometry algorithms. For the synthetic wavelength algorithm, these discontinuities are located equidistant from adjacent ideal phase lines. In this region, the spacing between adjacent ideal phase lines, $\Delta\phi_i$ is found by replacing $|\text{UR}_{\text{max}}|$ with Λ in Eq. 6. Thus, the values of \bar{m}_i are determined correctly when

$$|\delta\phi_{\perp}| < \pi \left(\frac{\lambda_a - \lambda_b}{\sqrt{\lambda_a^2 + \lambda_b^2}} \right). \quad (12)$$

This corresponds to the well-known condition: $|\delta\bar{m}_i| < 1/2$ [2, 15, 16], where $\delta\bar{m}$ is the error in \bar{m} before rounding to the nearest integer.

For an OPD in the region dominated by this condition, the synthetic wavelength algorithm has robustness given by

$$R = \left(\frac{1}{2\pi\sigma_a\sigma_b} \right) \int_{+\infty}^{-\infty} \int_{r_{\lambda}x - \frac{\Delta\phi_b}{2}}^{r_{\lambda}x + \frac{\Delta\phi_b}{2}} e^{-\frac{1}{2} \left(\frac{x^2}{\sigma_a^2} + \frac{y^2}{\sigma_b^2} \right)} dx dy. \quad (13)$$

When $\sigma_a = \sigma_b$, Eq. 13 is reduced to

$$R = \text{erf} \left(\frac{\Delta\phi_a \Delta\phi_b}{2\sigma\sqrt{2(\Delta\phi_a^2 + \Delta\phi_b^2)}} \right). \quad (14)$$

Near the edges of the OPD range, we see that the space between the ideal phase lines and the discontinuities begins to shrink. The change in the behavior of the algorithm is related to a second condition $|\phi_{e,0} + \delta\phi_e| = |\phi_{e,0} - \delta\phi_a + \delta\phi_b| < \pi$ where $\phi_{e,0}$ is the effective phase in the absence of error. Writing this constraint in terms of $\delta\phi_{\perp}$ gives

$$\left| 2\pi \frac{\tilde{d}}{\Lambda} - (\sin\theta + \cos\theta)\delta\phi_{\perp} \right| < \pi \quad (15)$$

where θ is defined in Eq. 9, and we've used Eq. 7 to rewrite the equation in terms of the measured OPD \tilde{d} , where $\tilde{d} = d_0 + \delta d$ and d_0 is the OPD in the absence of any parallel phase error ϕ_{\parallel} . In Fig. 3, these constraints are plotted across the entire UR for the synthetic wavelength algorithm when $\lambda_a = 700$ nm and $\lambda_b = 500$ nm.

As shown in Fig. 2, the interaction of these constraints can effectively partition the phase space in a non-uniform and uneven manner, making the correct determination of the values of \bar{m}_i much more challenging. In Sec. 7, we discuss the robustness of the algorithms presented in this paper in more detail (see Fig. 5 in Sec. 7 where the robustness of the synthetic wavelength algorithm over the UR of the algorithm is shown in comparison to the HC algorithm).

6 De Groot Algorithm

De Groot proposed an algorithm which extends the unambiguous range beyond that of the synthetic wavelength algorithm. To achieve this, de Groot's algorithm resolves the Λ ambiguity which will arise when applying the synthetic wavelength algorithm to range greater than $\pm\Lambda/2$ [1]. With this in mind, we note that the OPD may be written as

$$d = \Lambda(\bar{M} + \dot{M}). \quad (16)$$

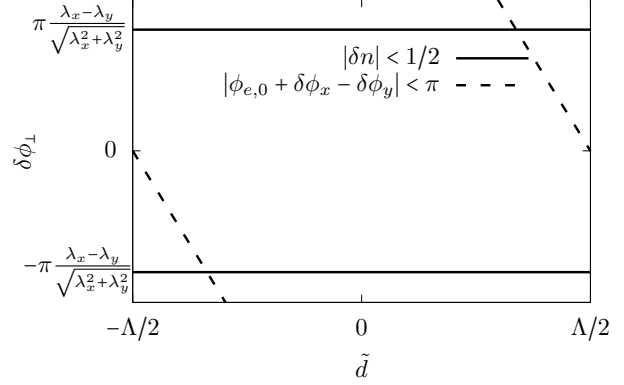


Figure 3: Phase error constraints for the synthetic wavelength algorithm. Note that these constraints agree with the discontinuities in Fig. 2. This can be visualized by “stitching” together the partitions of Fig. 2 so that the ideal phase lines forms a continuous straight line with increasing OPD.

We introduce a quantity which will prove important to the analysis of this algorithm

$$f_i = \left\lfloor \frac{1}{\Lambda/\lambda_i - \lfloor \Lambda/\lambda_i \rfloor} \right\rfloor. \quad (17)$$

It is straightforward to show that $f_a = f_b$ and $f > 2$ for all wavelengths. The UR of de Groot's algorithm may be written as $\text{UR} = \pm\Lambda \lfloor f \rfloor / 2$.

Following the procedure described in Sec. 5, we apply the de Groot algorithm to a raster scan of phase values in the phase space. When performing this analysis, we find that the algorithm exhibits qualitatively different behavior depending on the difference between f and the nearest integer value, given by $f - \lfloor f \rfloor$.

When $f - \lfloor f \rfloor = 0$, $f \in \mathbb{Z}$ and $\text{UR} = \pm\Lambda f / 2$. An example of the output of de Groot's algorithm when $f - \lfloor f \rfloor = 0$ is shown in Fig. 4a. In this scenario, de Groot's algorithm produces an even partitioning of the phase space. As with the synthetic wavelength algorithm, discontinuities in the algorithm's output are related to constraints on the phase error. For de Groot's algorithm, this constraint is

$$|\delta\bar{M}| < \frac{1}{2} \quad (18)$$

which may be rewritten in terms of $\delta\phi_{\perp}$ as

$$|\delta\phi_{\perp}| < \frac{\pi}{f} \left(\frac{\lambda_a - \lambda_b}{\sqrt{\lambda_a^2 + \lambda_b^2}} \right). \quad (19)$$

The maximum allowed $\delta\phi_{\perp}$ for de Groot's algorithm is smaller than the maximum $\delta\phi_{\perp}$ allowed by

the synthetic wavelength algorithm by a factor of f . However, de Groot's algorithm extends the UR of the synthetic wavelength algorithm by a factor of f . The inverse relationship between the maximum allowed $\delta\phi_{\perp}$ and the UR is a common feature to all algorithms since extending UR simply means that the bands of OPD continuity get more dense. In terms of UR/λ , both the basic synthetic wavelength algorithm and de Groot's algorithm are equally robust to phase error. However, unlike the synthetic wavelength algorithm, the robustness of de Groot's algorithm does not deteriorate near the edges of the UR.

The output of de Groot's algorithm becomes more complicated when $f - \lfloor f \rfloor \neq 0$. Eqs. (10-13) from de Groot's paper [1] feature rounding functions that are used to extend the UR. Each rounding function is a source of discontinuity in the algorithm's output. In Fig. 4 we relate the discontinuities in the algorithm's output to Eqs. (10-13) from Ref. [1] for different values of f .

While it is difficult to make general statements regarding the robustness of de Groot's algorithm, a few observations can be made. First, the robustness of de Groot's algorithm depends on OPD when $f - \lfloor f \rfloor \neq 0$. Second, when averaged over the entire UR, robustness decreases as $f - \lfloor f \rfloor$ moves further from zero.

7 Houairi & Cassaing Algorithm

An algorithm which achieves the maximum UR for a given choice of wavelengths was developed by Houairi and Cassaing [2]; we refer to this as the HC algorithm. The HC algorithm utilizes the arithmetic properties of the fundamental Diophantine equation relating phase measured by one wavelength to the phase measured by the other wavelength, as described in Sec. 2, to disambiguate the phases to a greater extent than the typical synthetic wavelength algorithm. Unlike the other algorithms examined in this paper, the spacing between discontinuities and the ideal phase lines for this algorithm remain constant over the entire UR. The HC algorithm will correctly resolve the values of \tilde{m}_i as long as the phase errors satisfy the constraint [2]

$$|-p\delta\phi_a + q\delta\phi_b| < \pi, \quad (20)$$

where p and q are as defined in Eq. 1, and also the constraint for the end of the UR as shown in Eq. 10. The constraint in Eq. 20 may also be rewritten in terms of $\delta\phi_{\perp}$ as

$$|\delta\phi_{\perp}| < \frac{\pi}{\sqrt{p^2 + q^2}}. \quad (21)$$

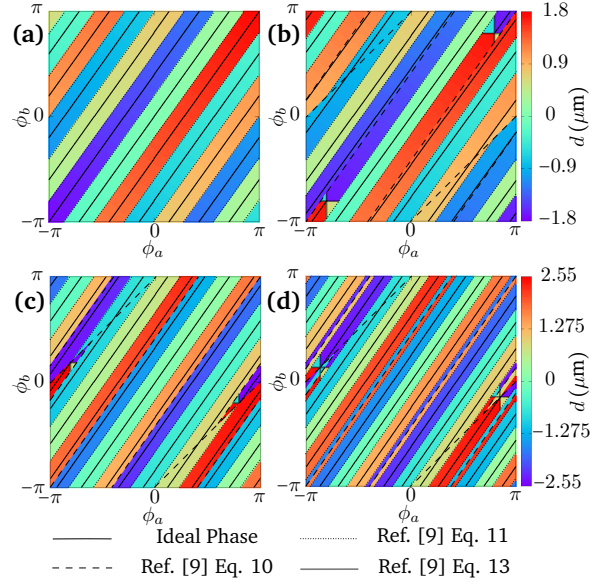


Figure 4: Output of de Groot's algorithm for (a) $f = 2.00$, (b) $f = 2.49$, (c) $f = 2.51$, and (d) $f = 3.49$. Note that these values of f are chosen to maximize the complex behavior of de Groot's algorithm when $f - \lfloor f \rfloor$ is far from zero. The wavelengths chosen are 500 nm and 700 nm, 500 nm and 708.194 nm, 500 nm and 708.472 nm, and 500 nm, 718.672 nm respectively. Each discontinuity is associated with an equation in de Groot's paper [1]. Note that some discontinuities are smaller than a wavelength, and, therefore, difficult to see. The rounding function in Ref. [1] Eq. (12) does not create discontinuities in the algorithm's output. The HC algorithm produces the same output as de Groot's algorithm for $\lambda_a = 700$ nm and $\lambda_b = 500$ nm. Unlike de Groot's algorithm, the HC algorithm always produces an even partitioning of the phase space. As a result, the HC algorithm will always produce an output similar to the figure in the top left.

Note that the HC algorithm is equivalent to de Groot's algorithm when $f - \lfloor f \rfloor = 0$. The robustness of the HC algorithm, calculated following the description at the end of Sec. 4, results in Eq. 13 or Eq. 14, where $\Delta\phi_i$ are given by Eq. 6. In Fig. 5 the robustness of the synthetic wavelength and HC algorithms are calculated and compared across the entire UR. Wavelengths $\lambda_a = 700$ nm and $\lambda_b = 500$ nm are used for the HC algorithm. For the synthetic wavelength algorithm, wavelengths $\lambda_a = 619.824$ nm and $\lambda_b = 526.572$ nm are used to achieve a similar UR and robustness near $d = 0$ as for the HC algorithm. Phase errors of $\sigma_a = \sigma_b = 0.0939$ radians are used

to calculate the robustness of both algorithms. From Fig. 5, we see the robustness of the synthetic wavelength algorithm deteriorates much sooner than the HC algorithm as $d \rightarrow \text{UR}$.

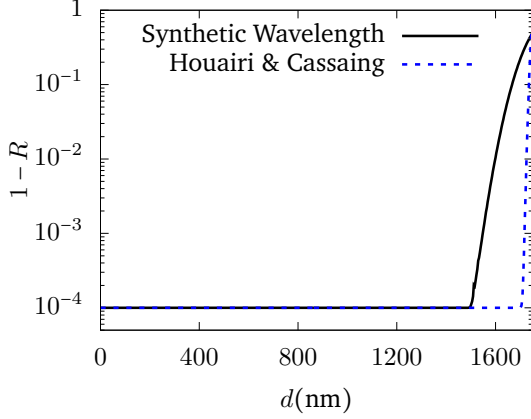


Figure 5: Comparison of algorithm robustness. HC algorithm uses $\lambda_a = 700$ nm, $\lambda_b = 500$ nm and $\sigma_a = \sigma_b = 0.0939$ radians. Synthetic wavelength algorithm uses $\lambda_a = 619.824$ nm, $\lambda_b = 526.572$ nm, and $\sigma_a = \sigma_b = 0.0939$ radians; these wavelengths were chosen to achieve the same UR and robustness of 0.9999 at $d = 0$.

8 Wavelength Error

We have thus far neglected wavelength error in this analysis. This is justified as phase errors are typically on the order of $\pi/100$ or worse. Meanwhile, locking and measuring a wavelength with a fractional uncertainty of $< 10^{-4}$ is relatively simple using commercial servos and wavemeters. Therefore, as we proceed, we will assume that errors in wavelength are small compared to the phase errors.

We denote the measured wavelength as $\tilde{\lambda}$, the actual wavelength as λ_0 and the error in the measured wavelength as $\delta\lambda$, so that $\tilde{\lambda} = \lambda_0 + \delta\lambda$. The output of any algorithm is determined by the user-specified measured wavelengths $\tilde{\lambda}_i$. Meanwhile, the ideal phase values, ϕ_0 , are determined by the actual wavelength λ_0 . We may conceptually understand the effects of wavelength error by plotting the ideal phase values across phase space, given by $\phi_{0,i} = 2\pi d/\lambda_{0,i} \bmod 2\pi$, against the OPD (d) from the HC algorithm using $\tilde{\lambda}_i$. This phase space representation presented in Fig. 6 shows that the slope of the ideal phase lines no longer match the slope of the discontinuities in the algorithm's output. As a result, ideal phase values move closer to one discontinuity and further from the

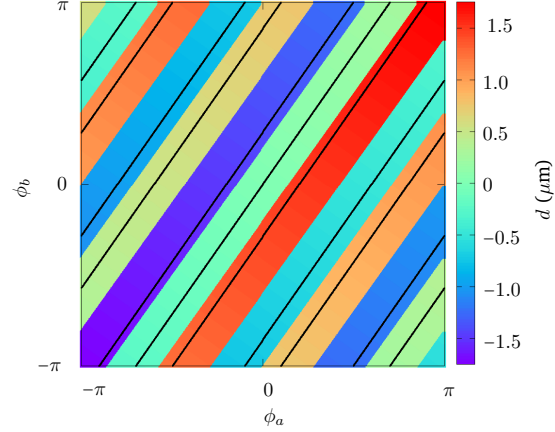


Figure 6: Output of the HC algorithm for $\lambda_{0,a} = 700$ nm and $\lambda_{0,b} = 500$ nm with ideal phase values for $\tilde{\lambda}_a = 714$ nm and $\tilde{\lambda}_b = 500$ nm.

other. This can be thought of as a systematic contribution to $\delta\phi_{\perp}$. The relationship between $\delta\lambda_i$ and the contribution to $\delta\phi_{\perp}$ caused by $\delta\lambda_i$, which we denote as $\delta\phi_{\lambda,\perp}$, is given by

$$\delta\phi_{\lambda,\perp} = 2\pi \left(\frac{\delta r_{\lambda}}{r_{\lambda}} \right) \frac{d}{\sqrt{\lambda_a^2 + \lambda_b^2}} \quad (22)$$

where $r_{\lambda} = \lambda_a/\lambda_b$, so that δr_{λ} is given by

$$\delta r_{\lambda} = \frac{\lambda_b \delta\lambda_a - \lambda_a \delta\lambda_b}{\lambda_b^2}. \quad (23)$$

When the phase uncertainty is the same for both phases and considering both phase and wavelength errors, the robustness of the HC algorithm is then given by

$$R \approx \frac{1}{2} \left(\operatorname{erf} \left(\frac{\pi \lambda_x \lambda_y}{\sigma |\text{UR}| \sqrt{2(\lambda_x^2 + \lambda_y^2)}} - \frac{\delta\phi_{\lambda,\perp}}{\sqrt{2}\sigma} \right) - \operatorname{erf} \left(-\frac{\pi \lambda_x \lambda_y}{\sigma |\text{UR}| \sqrt{2(\lambda_x^2 + \lambda_y^2)}} - \frac{\delta\phi_{\lambda,\perp}}{\sqrt{2}\sigma} \right) \right) \quad (24)$$

Fig. 7 demonstrates the robustness R from Eq. 24 resulting from either a small or a large error in one of the two wavelengths used for the HC algorithm.

9 Conclusions

In this paper we introduced the idea of the phase space as a tool for analyzing the behavior of multi-wavelength interferometry algorithms. We show that

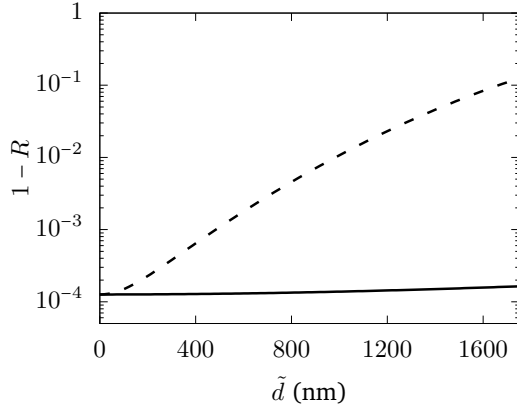


Figure 7: Robustness of the HC algorithm when for $\lambda_{0,a} = 700$ nm, $\lambda_{0,b} = 500$ nm and $\sigma_a = \sigma_b = 0.0939$ with wavelength errors: $\delta\lambda_a = 0$ nm and $\delta\lambda_b = 1$ nm (solid); $\delta\lambda_a = 0$ nm and $\delta\lambda_b = 14$ nm (dashed).

the component of the phase error perpendicular to the ideal phase lines is solely responsible for algorithm success. When the phase uncertainty is the same for both wavelengths, we find that the component of the phase error parallel to the ideal phase lines is responsible for error in the calculated OPD.

We note that the robustness of an algorithm which does not achieve the maximum UR will likely depend on the OPD. In particular, we show that the robustness of the synthetic wavelength algorithm decreases when the OPD is within $\lambda/2$ of $\pm\Lambda/2$. We show that the drop in robustness is associated with an overlooked constraint of the synthetic wavelength algorithm. We show that robustness of de Groot's algorithm depends on wavelength choice and OPD in a non-trivial way. Finally we show that the HC algorithm results in an optimal partitioning of the phase space. This even partitioning results in uniform robustness across the entire UR. We examined the effect of wavelength error on the robustness of the HC algorithm and found that wavelength errors result in robustness which decreases as $|d|$ increases.

Funding This work was funded by the Air Force Office of Scientific Research under lab task 22RV-COR017.

Disclaimer The views expressed are those of the authors and do not necessarily reflect the official policy or position of the Department of the Air Force, the Department of the Defense, or the U.S. Government.

References

[1] P. J. de Groot, *Appl. Opt.* **33**, 5948 (1994).

- [2] K. Houairi and F. Cassaing, *J. Opt. Soc. Am. A* **26**, 2503 (2009).
- [3] M. Chiaradia, L. Guerriero, G. Pasquariello, A. Refice, and N. Veneziani, in *IGARSS '96. 1996 International Geoscience and Remote Sensing Symposium*, Vol. 4 (1996) pp. 2060–2062 vol.4.
- [4] N. Veneziani, F. Bovenga, and A. Refice, *Multi-dimensional Systems and Signal Processing* **14**, 183 (2003).
- [5] J. Xu, D. An, X. Huang, and G. Wang, *IET Radar, Sonar & Navigation* **10**, 426 (2016).
- [6] T. Siebert, K. Splitthof, and A. Ettemeyer, *Journal of Holography and Speckle* **1**, 32 (2004).
- [7] D. Yankelev, C. Avinadav, N. Davidson, and O. Firstenberg, *Science Advances* **6**, eabd0650 (2020).
- [8] J. C. Wyant, B. F. Oreb, and P. Hariharan, *Appl. Opt.* **23**, 4020 (1984).
- [9] W. B. Ribbens, *Appl. Opt.* **13**, 1085 (1974).
- [10] C. Polhemus, *Appl. Opt.* **12** **9**, 2071 (1973).
- [11] K. Falaggis, D. P. Towers, and C. E. Towers, in *Interferometry XIV: Techniques and Analysis*, Vol. 7063, edited by J. Schmit, K. Creath, and C. E. Towers, International Society for Optics and Photonics (SPIE, 2008) pp. 318 – 325.
- [12] M. G. Lofdahl and H. Eriksson, *Opt. Eng.* **40**, 984 (2001).
- [13] H. van Brug and R. G. Klaver, *Pure & Appl. Opt.: J. Euro. Opt. Soc. A* **7**, 1465 (1998).
- [14] J. C. Wyant, *Appl. Opt.* **10**, 2113 (Sept. 1971).
- [15] K. Creath, *Appl. Opt.* **26**, 2810 (1987).
- [16] P. de Groot and S. Kishner, *Appl. Opt.* **30** (1991), 10.1364/AO.30.004026.